

## Preparation, structure and luminescence properties of the $Ln_{1-x}Ca_xVO_4$ , $Ln = La, Eu$ ( $0 \leq x \leq 0.2$ ) phases

Alina A. SLEPETS<sup>1\*</sup>, Tetiana A. VOITENKO<sup>1</sup>, Sergiy A. NEDILKO<sup>1</sup>, Sergiy G. NEDILKO<sup>2</sup>, Oksana V. CHUKOVA<sup>2</sup>

<sup>1</sup> Faculty of Chemistry, Taras Shevchenko National University of Kyiv, Volodymyrska St. 60, 03601 Kyiv, Ukraine

<sup>2</sup> Faculty of Physics, Taras Shevchenko National University of Kyiv, Acad. Hlushkova Ave. 4-b, 03680 Kyiv, Ukraine

\* Corresponding author. Tel.: +380-68-7600258; e-mail: giva@online.ua

Received September 25, 2016; accepted December 28, 2016; available on-line August 14, 2017

$Ln_{1-x}Ca_xVO_4$ ,  $Ln = La, Eu$  ( $0 \leq x \leq 0.2$ ) samples were prepared by the aqueous nitrate-citrate sol-gel route using citric acid as complexing agent. Thermal analysis was used to explain the thermal decomposition behavior and crystallization process of the  $Eu_{0.9}Ca_{0.1}VO_4$  sample. Single-phase samples of the investigated compounds formed at 630°C. According to X-ray diffraction data, a monoclinic phase of  $Ca^{2+}$ -doped  $LaVO_4$  and a tetragonal phase of  $Ca^{2+}$ -doped  $EuVO_4$  nanoparticles were obtained. Scanning electron microscopy images showed particles of different shapes with diameters from 100 to 500 nm, the crystallite surface being loose and porous. The photoluminescence spectra contain wide bands of matrix emission and narrow lines due to  $f-f$  transitions in the  $Ln^{3+}$  ions.

$Ca^{2+}$ -doped  $RVO_4$  / Nanoparticles / Sol-gel process / Thermal analysis / Scanning electron microscopy SEM

### Introduction

Alkaline-earth metal vanadates are important in various fields, including chemical and biological applications, luminescent devices and optical fibers. Vanadates exhibit unusual magnetic, optical, thermally-activated, and X-ray luminescence properties [1]. They present unique features and alternative technology and photocatalysis have recently attracted considerable attention. The most widely used photocatalyst  $TiO_2$  is only active under ultraviolet light irradiation [2,3]. Europium ( $EuVO_4$ ) [4] and lanthanum ( $LaVO_4$ ) [5] vanadates are of special interest, since they are among the most promising visible-light-driven photocatalysts [6]. These compounds also offer chemical stability and non-toxicity. They have been used in a range of biological applications, such as fluorescent probes for single-molecule tracking, drug development, protein detection and fluorescent bio-labeling [7,8].

The search for new rare-earth orthovanadates leads to “created” cations, including partial substitution  $Eu^{3+}/Ca^{2+}$  and  $La^{3+}/Ca^{2+}$ . The aim of this work was to study the conditions of synthesis of the  $Ln_{1-x}Ca_xVO_4$ ,  $Ln = La, Eu$  ( $0 \leq x \leq 0.2$ ) phases and to investigate their structural features, as well as their morphological and physical properties.

There exist different methods to obtain vanadate particles, such as solid-state or [9] hydrothermal synthesis [5], sol-gel method [10], etc. One of the most promising ways to obtain excellent homogenization at the atomic scale and high reactivity, is the sol-gel method.

### Experimental

The  $Ln_{1-x}Ca_xVO_4$ ,  $Ln = La, Eu$  ( $0 \leq x \leq 0.2$ ) samples were prepared by the aqueous nitrate-citrate sol-gel synthesis route taking citric acid (CA) as complexing agent, as shown in Fig. 1. Lanthanum(III) and europium(III) nitrates,  $La(NO_3)_3$ ,  $Eu(NO_3)_3$ , calcium(II) nitrate,  $Ca(NO_3)_2$ , and ammonium metavanadate,  $NH_4VO_3$ , were used as starting materials and weighed according to the desired stoichiometric ratio. Nitric acid ( $HNO_3$ ), distilled water and ammonia ( $NH_3 \cdot 4H_2O$ ) were used as solvents and reagents to regulate the pH of the solutions. Firstly  $NH_4VO_3$  was dissolved in a concentrated ammonia solution by stirring at 70-80 °C. Then the CA, dissolved in distilled water with a small amount of  $NH_3 \cdot 4H_2O$ , was added. Next,  $La(NO_3)_3$ ,  $Eu(NO_3)_3$ , and  $Ca(NO_3)_2$  were added. To prevent precipitation, the pH was controlled and

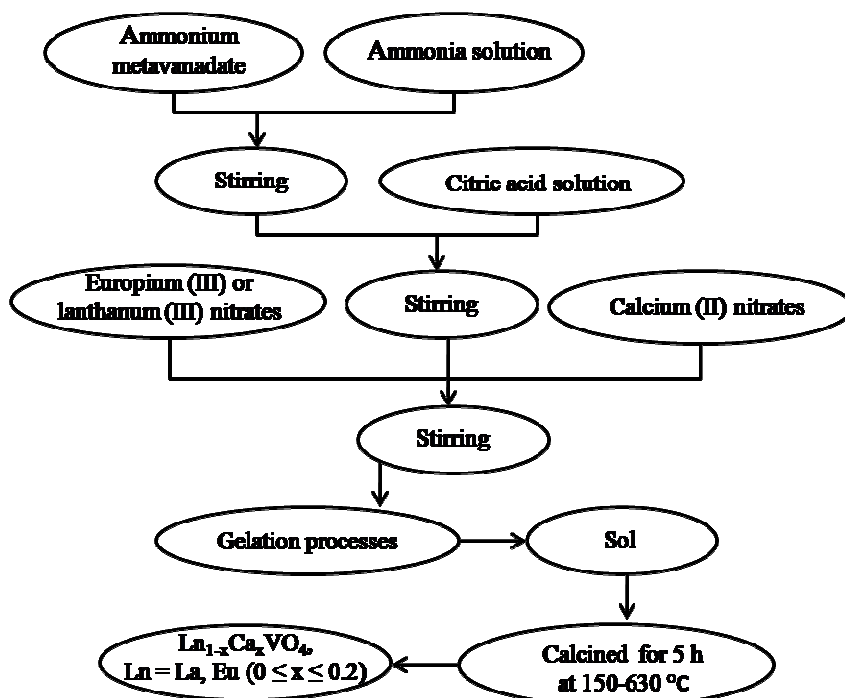


**Fig. 1** Flow-chart for the preparation of orthovanadates by the sol-gel method.

maintained at a value of  $\sim 6-7$ . Finally, the same amount of aqueous solution of the complexing agent CA was repeatedly added to the reaction mixture to prevent crystallization of metal salts during the gelation process. The clear solution was concentrated by slow evaporation at  $80-90^\circ\text{C}$  in an open beaker. A transparent gel formed when nearly 90 % of the water had been evaporated under continuous stirring. After drying in an oven at  $100^\circ\text{C}$ , a sol was obtained. The sol was calcined for 5 h at 150, 300, or  $450^\circ\text{C}$  and carefully reground in an agate mortar. After grinding, the obtained powders were repeatedly annealed for 5 h at 500 and  $630^\circ\text{C}$ .

Thermal measurements were performed with a TG-DTG MOM Q-1000 device in the temperature range  $150-800^\circ\text{C}$  at a heating rate of  $20^\circ\text{C min}^{-1}$  with a sample mass of about 5 mg.

Infrared spectra (IR) of the samples were recorded on a PerkinElmer IR spectrometer using the KBr pellet method in the range  $1400-400\text{ cm}^{-1}$ .

The phase composition and crystal lattice parameters were determined using X-ray diffractometers DRON-3M ( $\text{Cu } K_\alpha$ -radiation with a Ni filter) and DRON-7 ( $\text{Fe } K_\alpha$ -radiation with a Mn filter). The diffraction patterns were taken with a step of  $2\text{ deg./min}$ .

The microstructures of the compounds were studied by a scanning electron microscope (SEM) Hitachi S-2400.

Photoluminescence of the  $Ln_{1-x}Ca_xVO_4$ ,  $Ln = La, Eu$  ( $0 \leq x \leq 0.2$ ) samples was observed in the visible range  $350-600\text{ nm}$ . The measurements were carried out

at the Laboratory “Spectroscopy of condensed matter” at the Faculty of Physics, Taras Shevchenko National University of Kyiv.

## Results and discussion

Thermal analysis (TG-DTG) was performed to study the thermal decomposition behavior and crystallization process of the synthesized  $Ln_{1-x}Ca_xVO_4$ ,  $Ln = La, Eu$  ( $0 \leq x \leq 0.2$ ) samples. The curves for the  $\text{Eu}_{0.9}\text{Ca}_{0.1}\text{VO}_4$  sample are shown in **Fig. 2**.

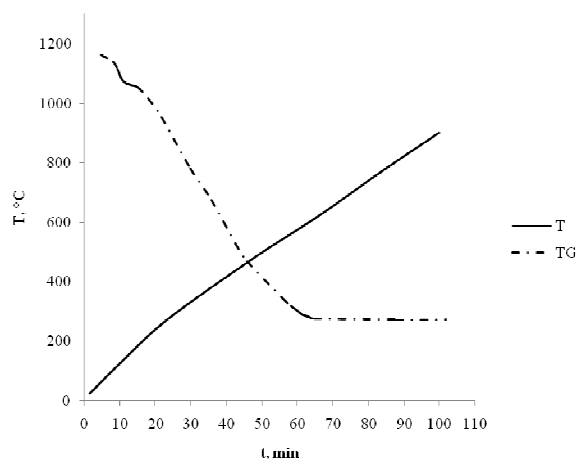


**Fig. 2** Thermal analysis of the  $\text{Eu}_{0.90}\text{Ca}_{0.10}\text{VO}_4$  sample.

The first mass loss in the TG curve ranges from 40 to 150°C and corresponds to the removal of water adsorbed on the surface of the sample. By further increasing the temperature from 150 to 200°C the mass of the sample was decreased. This can be the result of the initial decomposition of citric acid and metal nitrates. Finally, the last mass loss observed between 200 and 630°C accords with the decomposition of citric acid or metal citrates and nitrates, the intermolecular rearrangement of organic compounds, and the burning of carbon. On further increasing the

temperature, no further mass losses were observed in the TG curve.

The TG analysis of the  $Eu_{0.9}Ca_{0.1}VO_4$  sample suggests that a single-phase crystalline compound should form at 630°C.

IR-spectroscopy was performed to confirm the synthesis of  $Ln_{1-x}Ca_xVO_4$ ,  $Ln = La, Eu$  ( $0 \leq x \leq 0.2$ ). The results agree with the IR-spectra of  $Ln_{1-x}Ca_xVO_4$ ,  $Ln = La$  produced by solid state reaction [9].

The  $Ln_{1-x}Ca_xVO_4$ ,  $Ln = La, Eu$  ( $0 \leq x \leq 0.2$ ) compounds were identified by X-ray diffraction (XRD); the diffraction patterns are shown in Fig. 3.

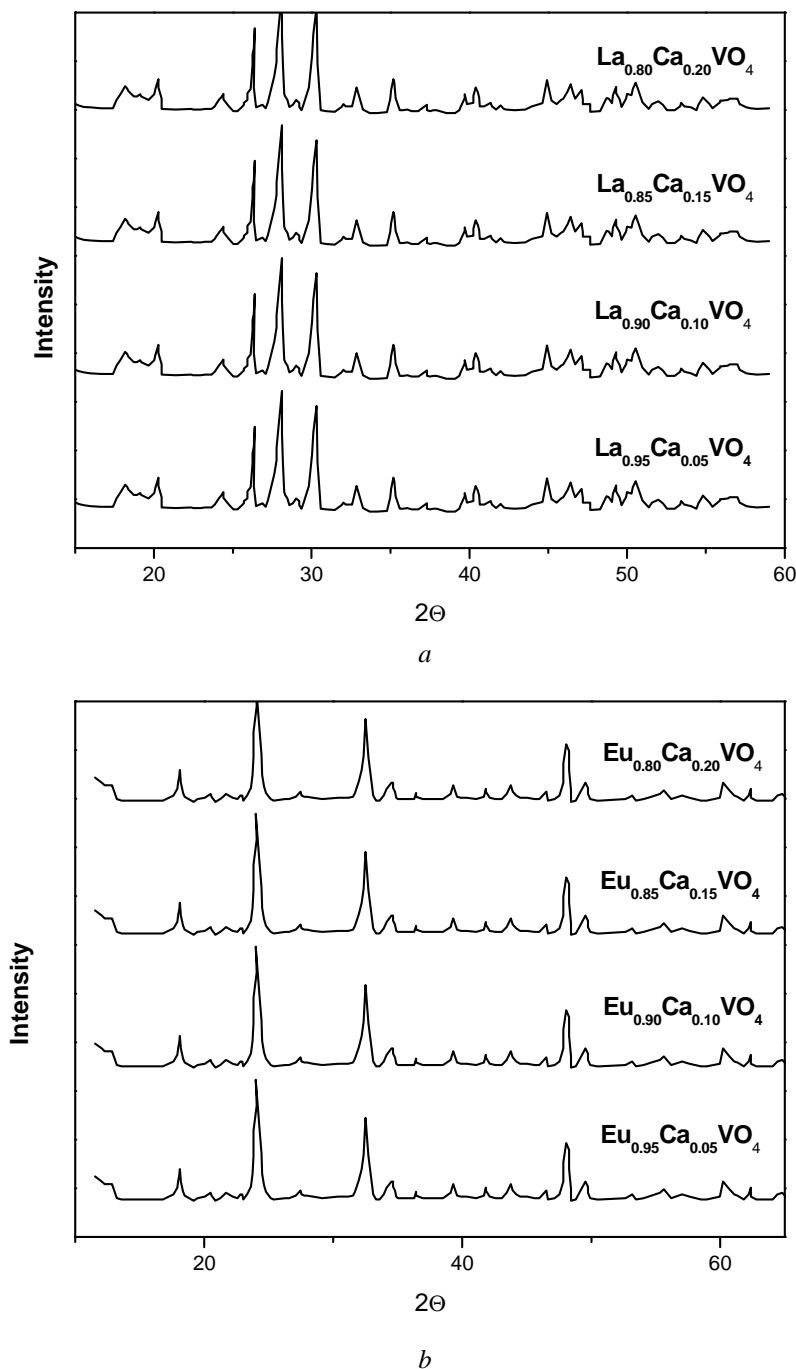


**Fig. 3** X-ray diffraction patterns of a)  $LaVO_4:Ca^{2+}$  and b)  $EuVO_4:Ca^{2+}$  nanoparticles.

In general, vanadate compounds crystallize in two polymorphs: the tetragonal zircon type (space group  $I4_1/amd$ ,  $Z = 4$ ) and the monoclinic monazite type (space group  $P2_1/n$ ,  $Z = 4$ ) [11]. Compounds with small rare-earth cations, such as  $EuVO_4$ , have zircon-type structure, whereas compounds with a large rare-earth cation, such as  $LaVO_4$ , will experience zircon to monazite phase transitions. However, the zircon-type structure of the  $LaVO_4$  compound is metastable [9]. The unit cells refined to  $a = 0.7043(1)$  nm,  $b = 0.7283(2)$  nm,  $c = 0.6723(2)$  nm,  $\beta = 104.855(3)^\circ$  for  $LaVO_4$  (monazite type),  $a = b = 0.7265(3)$  nm and  $c = 0.6383(1)$  nm for  $EuVO_4$ .

The patterns of the  $Ca^{2+}$ -doped  $LaVO_4$  particles fit well with the monoclinic phase of pure  $LaVO_4$  (JCPDS card no. 50-0367). Similar results were obtained for  $Ca^{2+}$ -doped  $EuVO_4$ , which give crystal structures in agreement with those reported in the literature (JCPDS card no. 15-0809).

The morphology of the synthesized powders and the size of the particles (that may consist of one or several crystallites) were studied using scanning electron microscopy (SEM). The SEM images (Fig. 4) show particles of different shapes, with diameters of 100-500 nm; the crystallite surface is loose and porous.

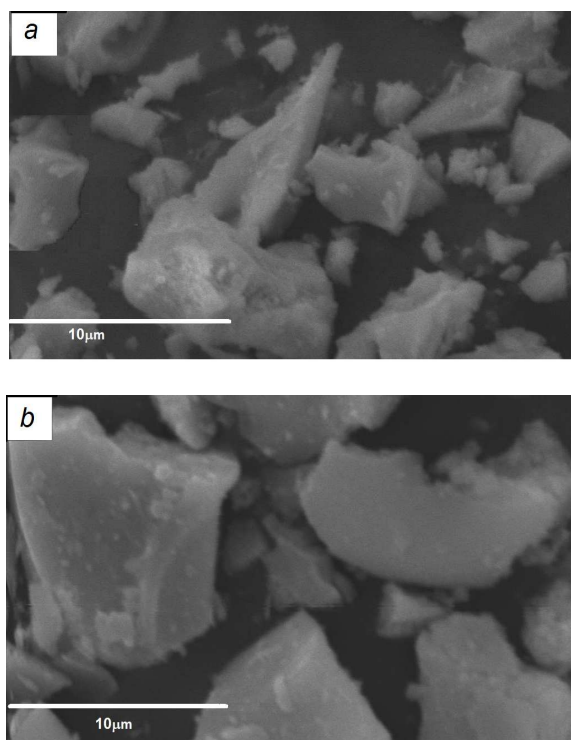


**Fig. 4** SEM images of the a)  $La_{0.90}Ca_{0.10}VO_4$  and b)  $Eu_{0.90}Ca_{0.10}VO_4$  samples.

The photoluminescence (PL) properties of the synthesized samples were investigated. The PL spectra contain wide bands of matrix emission and narrow lines caused by  $f-f$  transitions in the  $Ln^{3+}$  ions. The  $Eu^{3+}$  ions produce two types of emission center: the type I centers are formed by  $Eu^{3+}$  ions at their regular positions in the crystal lattice, whereas the type II centers have complex structure and consist of  $Eu^{3+}$  ions,  $Ca^{2+}$  cations and oxygen vacancies. The incorporation of  $Ca^{2+}$  ions into the  $EuVO_4$  lattice increases the intensity of the  $Eu^{3+}$  ion luminescence up to  $x = 0.15$ . The increase rate of the luminescence intensity is higher for the type II centers.

## References

- [1] Y. Zhang, G. Li, X. Yang, H. Yang, Z. Lu, R. Chen, *J. Alloys Compd.* 551 (2013) 544-550.
- [2] D. Wang, R. Li, J. Zhu, J. Shi, J. Han, X. Zong, C. Li, *J. Phys. Chem. C* 116 (2012) 5082-5089.
- [3] W. Li, D. Li, Y. Lin, P. Wang, W. Chen, X. Fu, Y. Shao, *J. Phys. Chem. C* 116 (2012) 3552-3560.
- [4] A.B. Garg, D. Errandonea, *J. Solid State Chem.* 226 (2015) 147-153.
- [5] X. Cheng, D. Guo, S. Feng, K. Yang, Y. Wang, Y. Ren, Y. Song, *Opt. Mater.* 49 (2015) 32-38.
- [6] V. Tamilmani, K.J. Sreeram, B.U. Nair, *RSC Adv.* 4 (2014) 4260-4268.
- [7] G. Mialon, M. Gohin, T. Gacoin and J.-P. Boilot, *ACS Nano* 2 (2008) 2505-2512.
- [8] J. Zhang, C. Mi, H. Wu, H. Huang, C. Mao, S. Xu, *Anal. Biochem.* 421 (2012) 673-679.
- [9] A. Slepets, T. Voitenko, S.A. Nedilko, S.G. Nedilko, O. Chukova, V. Scherbatsky, *Visn. Lviv. Univ., Ser. Khim.* 57 (2016) 122-127.
- [10] N. Chumha, S. Kittiwachana, T. Thongtem, S. Thongtem, S. Kaowphong, *Ceram. Int.* 40 (2014) 16337-16342.
- [11] C.E. Rice, W.R. Robinson, *Acta Crystallogr. B* 32 (1976) 2232-2233.